Journal of Nuclear Materials 398 (2010) 238–243

Contents lists available at ScienceDirect

Journal of Nuclear Materials

journal homepage: www.elsevier.com/locate/jnucmat

Development of JSNS target vessel diagnosis system using laser Doppler method

M. Teshigawara *, T. Wakui, T. Naoe, H. Kogawa, F. Maekawa, M. Futakawa, K. Kikuchi

Japan Atomic Energy Agency, Tokai-mura, Ibaraki-ken 319-1195, Japan

A B S T R A C T

When an intense pulsed proton beam with a power of 1 MW is irradiated to a mercury target, a pressure wave caused by the proton beam gives a vibration on the target vessel. Pitting damage also occurs on the target vessel, especially incident beam area, resulting in shortening of a life-time. It is very important to monitor the vibration of the target vessel from the view point of the life-time estimation. We developed the target vessel diagnosis system using laser Doppler method and successfully installed it in an actual pulsed spallation source. The diagnosis system consists of retro-reflecting corner-cube mirror (reflective mirror) on the target, mirror assembly in a reflector plug and laser source-detector. The newly developed reflective mirror, made by nickel, was installed by vacuum silver brazing on the target vessel to detect the target vibration. In order to pass the laser beam to the target vessel, a mirror assembly was installed inside the reflector plug. It is replaceable using a remote handling machine during a maintenance period. Nd-YAG laser beam (wave length: 533 nm) with the power of 50 mW was adopted to detect the target vibration. The first proton beam to the target in the spallation neutron source (JSNS) was provided on 30 May 2008. The first signal related to the target vibration was also detected by using this target vessel diagnosis system.

1. Introduction

The Japanese spallation neutron source (JSNS) is one of the main facilities in J-PARC (Japan Proton Accelerator Research Complex) project [1–3]. An intense pulsed proton beam with a power of 1 MW is irradiated to a mercury (Hg) target to produce neutrons for JSNS users. Pressure waves [4–7] generated in Hg by the intense short-pulse proton beam, propagate to the target vessel, resulting in vibration of the vessel. Pitting damage caused by the pressure waves becomes an issue for damaging the target vessel. As a result of off-line beam experiment, we could extrapolate that the pitting damage remarkably reduce the life-time of the target vessel [8–11] especially in the intense proton with roughly more than 16 kW/pulse, which corresponds to 3×10^{13} protons at 3 GeV/pulse [9], though it also depends on the beam profile such as a peak current density. In order to mitigate the pressure wave, R & D such as a bubble injection technique, is being developed under the international collaboration of JAEA (Japan Atomic Energy Agency) and ORNL (Oak Ridge National Laboratory). On the other hand, it is also important to establish the integrity evaluation of the target vessel in judgment of appropriate replacement of target vessel, but a technique still has not been established in the existing spallation sources. In order to develop the target vessel integrity evaluation, we focus on a measurement of the vibration generated by the pressure wave. An accelerometer and a strain gauge has been already utilized to detect the vibration, however, such vibrometers are not suitable for under the high neutron radiation field such as several DPA (displacement per atom)/year. We adopted a laser Doppler vibrometer with the advantage of being non-contact system. It prevents the sensor from the radiation damage. However, such a system has not been utilized in the existing source yet. In general, a precise alignment is indispensable for a laser vibrometer. However, it is impossible to align or re-align precisely in the high radiation fields. We introduced and developed the corner-cube retro-reflector (reflective mirror) for the transmitter of the target vessel vibration. It has concave corners (three mutually-orthogonal-mirror surfaces) like an inverted pyramid shape that reflect a laser light back to its source. This makes it very useful in applications where precise alignment is difficult to achieve, which means no-need of alignment. Only a metal based reflective mirror is feasible under a high radiation field. The smallest commercial size of the concave reflective mirror is available around 2–3 mm in base size. Almost one order of magnitude smaller is required (the base size: around 200 μm) for our application. More than ten by ten concaves at least should be viewed within the opening (around 2 mm in the smallest case) in the laser beam path between vessel components such as moderator and reflector to get enough returning beam intensity. Finally, the requirement for the development of the reflective mirror was decided as follows: (1) size: more than 10 mm × 10 mm, (2) thickness: less than 2 mm, (3) concave corner: three mutually-orthogonal-mirror surfaces, (4) base size of concave corner: around 200 μm under the condition of the tolerance of target fabrication (less than ±2 mm), installation (less than

* Corresponding author. Tel.: +81 29 282 6074; fax: +81 29 282 6496.
E-mail address: teshigawara.makoto@jaea.go.jp (M. Teshigawara).

0022-3115/$ - see front matter © 2009 Elsevier B.V. All rights reserved.
doi:10.1016/j.jnucmat.2009.10.038

±2 mm), clearance (less than 5 mm), etc. Available technologies did not offer a machining technique to make a concave corner with the base size of sub-millimeter directly on the surface. We developed the reflective mirror with many small concaved corners (base size: around 200 μm) by adopting indirect machining method using convex machining and electroforming. The target vessel diagnosis system could be installed for the first time in an actual pulsed spallation source by development of the reflective mirror.

In this paper, we report the development of target vessel diagnosis system enabled by the reflective mirror, and present measured data brought by proton beam bombardment and analysis.

2. Target vessel diagnosis system

Target vessel diagnosis system was installed at the pulsed neutron source, JSNS. The target vessel diagnosis system consists of a laser source-detector, an *X–Y* stage, a mirror assembly in the reflector plug and a retro-reflecting corner-cube mirror (reflective mirror) on the target as shown in Fig. 1.

2.1. Laser

Nd-YAG green laser (wave length: 533 nm) with power of 50 mW (Onosokki LV1720A) was adopted to monitor the vibration on the target vessel. A laser beam was introduced into the top of core vessel of neutron source using the polarization-preserving single-mode optical-fiber with the length of ca. 30 m. It was emitted from the end of the optical-fiber into helium (He) environment in the core vessel. A beam profile was TEM00 with 10 mm in diam. at the emitted position. The beam was incident upon the reflective mirror on the target vessel through the ditch with the two bending parts inside a reflector plug from top of the core vessel. The bending positions were provided to reduce neutron streaming, bringing about low activation at the top of the core vessel for rad-worker at the maintenance period. The beam was focused on the reflective mirror with 2 mm in diameter.

2.2. X–Y stage

An *X–Y* stage (KOHZU SC200) was installed at the top of the core vessel to control the beam axis as shown in Fig. 2. It includes two alignment pins to re-install them with an accuracy of ±0.5 mm. It also has an adjustor of ±20 mm with the resolution of 0.5 μm in the *X* or *Y* axis, which is operated by a pulse motor with radiation resistance of 1 MGy.

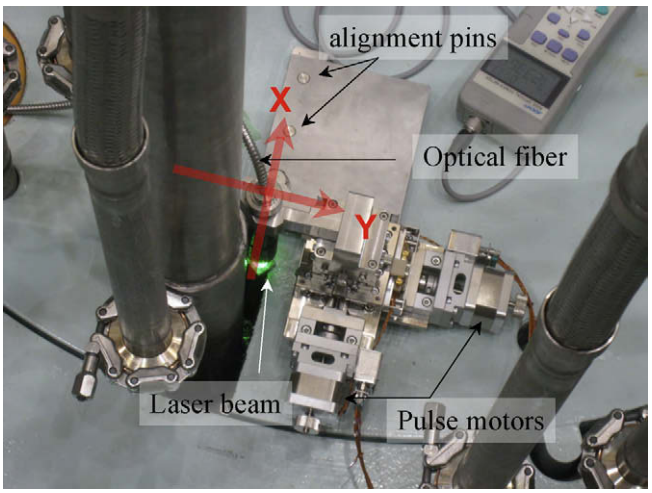

Fig. 2. *X–Y* stage. It is installed at the top of core vessel to control the laser beam axis using two alignment pins. Laser beam is emitted from end of the optical-fiber into the core vessel. Adjustment length is ±20 mm with the resolution of 0.5 μm/pulse in the *X* or *Y* axis, which is operated by pulse motor.

2.3. Mirror assembly

In order to travel the laser beam inside the reflector plug, mirror assembly was installed along the ditch of the reflector plug, which had two bending positions. Four triangular-aluminum(Al)-prism-mirrors were installed at the bending positions on the assembly as shown in Fig. 3. Al-prism-mirror with the size of $10 \times 14 \times 11\ mm^3$ was polished until less than 0.01 μm Ra in the roughness and coated 200 nm by magnesium fluoride (MgF_2) as an optical coating. The reflectance was observed more than 93% for each prism-mirror. The mirror assembly includes the two-alignment-pins to re-install with an accuracy of ±0.5 mm. It also has the adjustable jigs for each prism mirror to align a laser beam axis in the off-line. A template was also prepared to replace a new mirror assembly taking

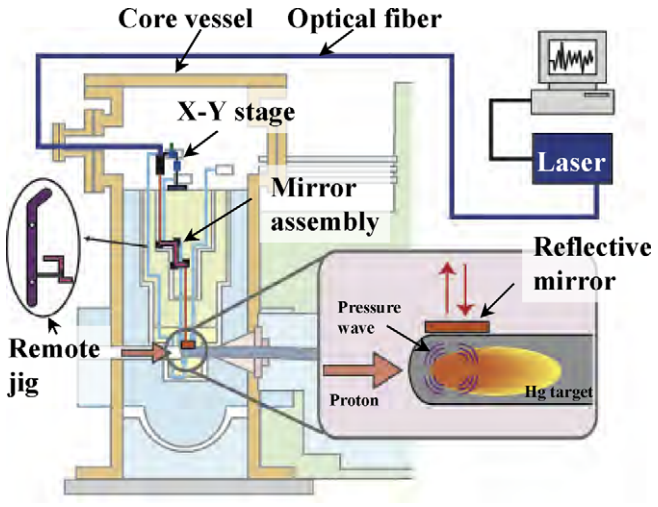

Fig. 1. Target vessel diagnosis system. It consists of retro-reflecting corner-cube mirror (reflective mirror) on the target, mirror assembly in the reflector plug, *X–Y* stage and laser source-detector.

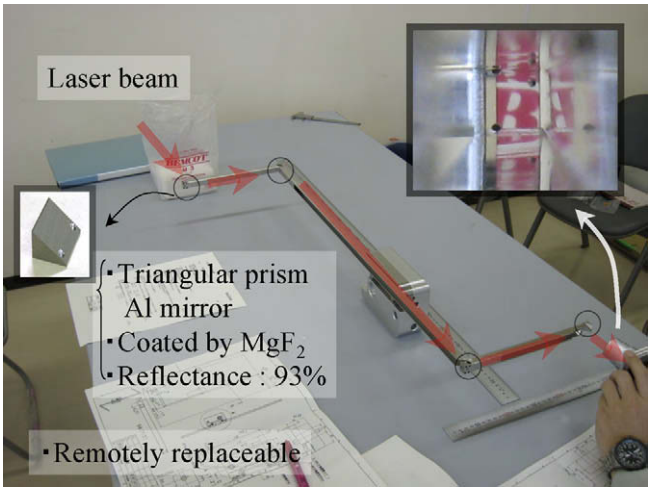

Fig. 3. Mirror assembly. Four triangular-aluminum(Al)-prism-mirrors were installed on mirror assembly. Al-prism-mirror is polished until less than 0.01 μm Ra in the roughness and coated 200 nm by magnesium fluoride (MgF_2), resulting in 93% reflectance. Character "B" can be seen in picture which is taken by camera from opposite side. It can be replaceable remotely in hot-cell.

into account the performance lost such as deterioration of reflection due to the neutron-radiation-damage, etc. In the commissioning process, the replacement test was also performed by using the remote handling machine in the hot-cell.

2.4. Corner-cube retro-reflection (reflective mirror)

2.4.1. Fabrication of reflective mirror

As we adopted the electroforming in the fabrication process of the reflective mirror, an available mirror material was only nickel (Ni) in terms of bonding the stainless steel (SS316L) of the target vessel. The fabrication process of the reflective mirror is shown in Fig. 4. A computer-numerical-control micro milling machine enabled to make many small-convex-triangular-pyramids (base size: ca. 200 μm) with three mutually perpendicular surfaces on the stainless steel plate, which was a substrate in the electroforming. The nickel was piled up to about 2 mm in the thickness on the milled stainless plate by the electroforming. Fig. 5 shows the reflective mirror, which was made by pure Ni. The roughness on the mirror surface was about 0.05 μm in Ra, which was measured by using a laser microscope (KEYENCE, VK-9510) under the condition of JIS B0601:2001. The reflectance of the mirror was 12.4%. Nd-YAG laser (533 nm) was used for the reflectance measurement. A no-reflection part was partly found in the corner because of the poor machining. The performance of mirror, such as response for the vibration and a retro-reflecting angle was measured using the MIMTM [9], which has an electro-magnetic forced vibration source. For the reference, it was compared to the commercially available retro-reflecting polymer mirror. The measured response was similar to that of the polymer one as shown in Fig. 6. Noise in measured response data was increasing at angle of more than 40°. It was confirmed that the angle of less than 15° gave the sufficient response signal as also shown in Fig. 6.

2.4.2. Brazing

It is required that the reflective mirror, which is made by Ni, is stuck on the target vessel (SS316L) to propagate the vibration of target vessel to the mirror directly. In order to join the Ni and SS316L plate, we did not adopt a soldering, but a vacuum-brazing because of significant advantages such as, extremely clean, flux-free braze joints of high integrity and strength. Candidate brazing material is an Al, silver (Ag) or gold (Au) based one, which has different brazing treatment temperatures. We only succeeded to have the joining plate of Ni and SS316L in case of Ag and Au based brazing materials as shown in Fig. 7. The treatment temperature for Ag and Au brazing materials were 1073 K and 1273 K, respectively.

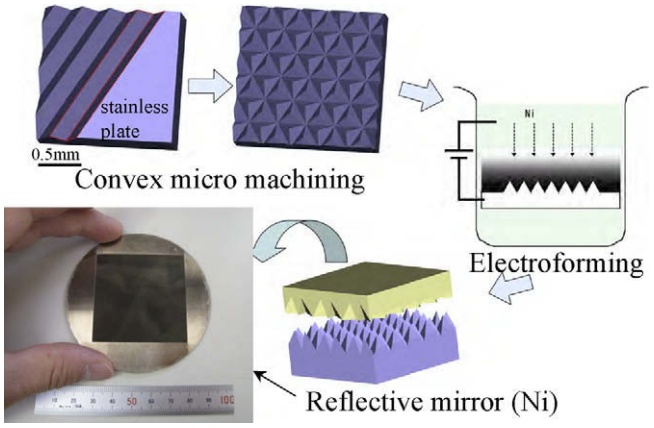

Fig. 4. Fabrication process of reflective mirror. Indirect machining method (convex machining and electroforming) is adopted to make the reflective mirror with many small-concave-corners. Many small convex-triangular-pyramids (base size: ca. 200 mm) with three mutually perpendicular surfaces on the stainless steal plate were made by computer-numerical-control micro milling machine. The nickel was piled up to about 2 mm by the electroforming.

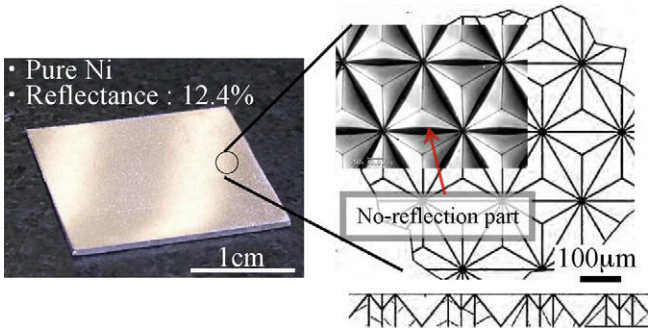

Fig. 5. Retro-reflecting corner-cube mirror (reflective mirror). In direct machining was adopted to make the concave corner with base size of 200 μm. It is made by pure Ni. The roughness on the surface was about 10 nm. The reflectance of this mirror was 12.4%. A no-reflection part was partly found in the figure because of poor machining.

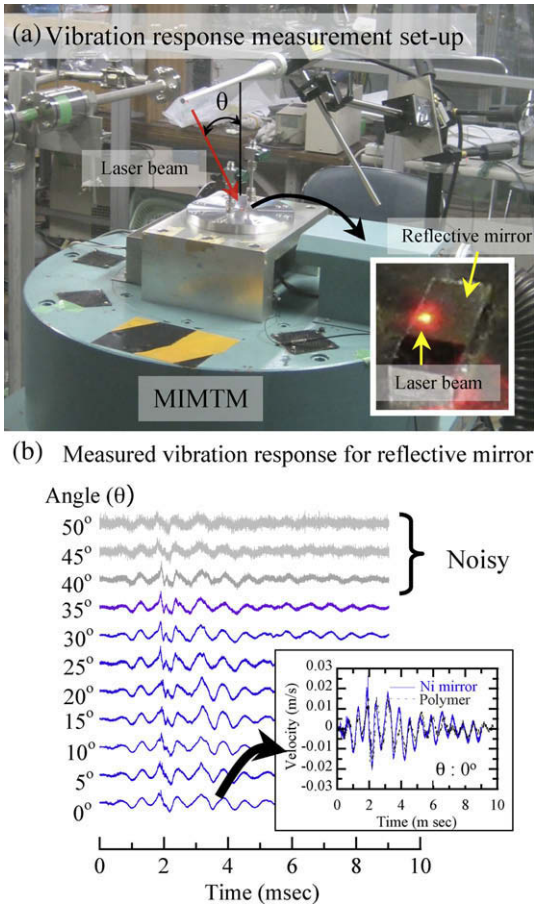

Fig. 6. Response measurement in vibration and retro-reflecting angle using MIMTM. Laser beam with varied incident angle was irradiated to reflective mirror, which was put on the vibration surface of MIMTM (a). For the reference, it was compared to the commercially available retro-reflecting polymer mirror. The measured response was similar to that of the polymer. Noise in measured response data was increasing more than angle of 40° (b).

2.4.3. Reduction of reflection in brazing process

Reflection of reflective mirror was reduced in the brazing process. It was due to the re-crystallization of Ni, which increased

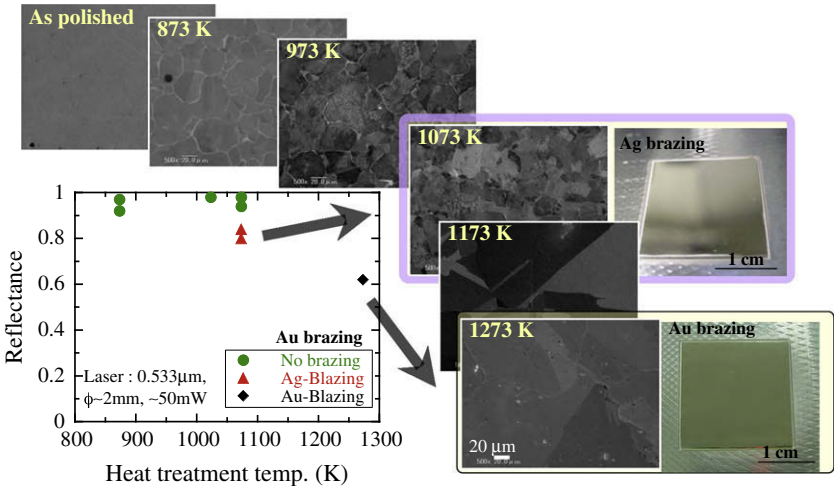

Fig. 7. Reduction of reflectance for the heat treatment in the brazing process. Reflection of reflective mirror was reduced in the brazing process. It was due to the re-crystallization of Ni, which increased the diffused reflection on the mirror surface. Higher temperature brazing treatment also gave more reduction of reflectance as shown in figure, especially, down to 62% in the Au brazing process.

the diffused reflection on the mirror surface. It can be seen that the grain size of Ni plate surface increased with high temperature as shown in a SEM (scanning electron microscopy) picture of Fig. 7. For the reflection measurement, a Ni plate was polished by using an alumina (Al_2O_3, ca. 1 mm in diam.) paste to achieve a mirror finish before brazing heat treatment. Higher temperature brazing treatment also gave more reduction of reflection as shown in Fig. 7, especially, down to 62% in the Au brazing process. That is why Ag based brazing process was adopted in the installation of the actual target vessel.

2.4.4. Installation of reflective mirror on target vessel

The reflective mirror was installed on the part of target vessel by vacuum Ag brazing as shown in Fig. 8b. A thin film (50 μm) of JIS BAg-8 brazing material (72Ag–28Cu, eutectic) was inserted between mirror and target vessel in the vacuum-brazing process. The Ag brazing condition is shown in Table 1. It can be seen that the brazing material partially went up to the edge of the mirror as shown in Fig. 8c, but it did not affect on the main reflection area. Reduction of reflection was measured in the main reflection area.

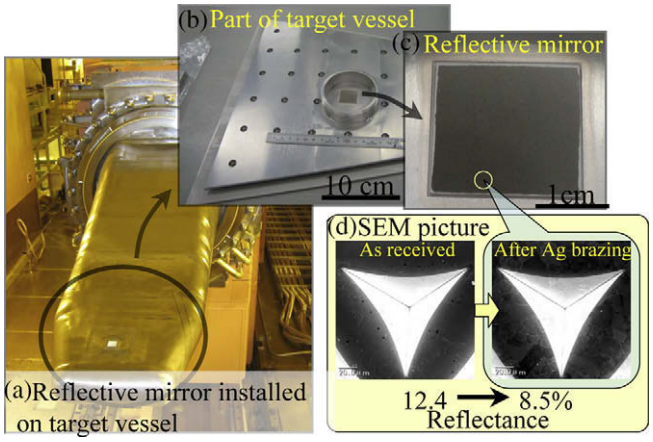

Fig. 8. Installation of reflective mirror on target vessel. Reflective mirror was installed on the part of target vessel by vacuum Ag brazing (b). It can be seen that the brazing material partially went up to the edge of mirror (c). Reflection loss was measured in the main reflection area. It was down to 8.5%. The re-crystallizing was also found (d). The reflective mirror was finally assembled by using bolts and welding to the target vessel (a).

Table 1
Ag brazing conditions for installation of reflective mirror on the target vessel.

Brazing material	JIS BAg-8, 72Ag–28Cu
Pre-heating temp	1033 K (90 min holding)
Brazing temperature	1073 K (40 min holding)
Increasing temperature	10 K/min
Decreasing temperature	Natural cooling
Vacuum condition	1.3×10^{-3} Pa

It was down to 8.5% after Ag brazing process. The re-crystallizing was also found as shown in Fig. 8d. The roughness of the mirror surface was measured, resulting in about 0.31 μm in Ra. It was about 6 times larger than that of before brazing process. This part was finally assembled to the target vessel by using bolts and welding as shown in Fig. 8a. The welding positions to fabricate the vessel were separated 5 cm at least from the reflective mirror to avoid the heat effect on the reflectance of the mirror and the brazing treatment as shown in Fig. 8b.

2.4.5. Total performance of reflectivity

Finally, the returned-laser-beam was detected from the target vessel surface at the laser beam incident position. The beam power was 4–7 μW, which corresponded to about 1/50 of initial beam power. This value corresponded to the design one.

2.5. Data acquisition

Windows XP operation system based computer (CPU: Intel Core 2 Duo, Mem: 1 GB) included A/D converter (National Instruments NI PCI-6132) was used for the data acquisition. The reflective memory (GE Fanuc Automation VMIPCI-5665-01000) was installed in the computer to get the identified number supplied from the master clock for each proton beam pulse. It has a Disk Array giving two TB storage-capacities, resulting in about 7 day measurement period (Sampling rate: 1 MHz, Sampling time: 20 ms, Repetition: 25 Hz, Frequency range: less than 200 kHz). We also performed an off-beam-line-experiment to confirm the time response of the data acquisition. A different propagation speed detection of wave motion (longitudinal or transverse wave) was used for the time response measurement. Different sensors (strain gauge and reflective mirror for the laser vibrometer) were arranged at same position on a hollow-pillar-steel-rod so as to detect the different wave motion

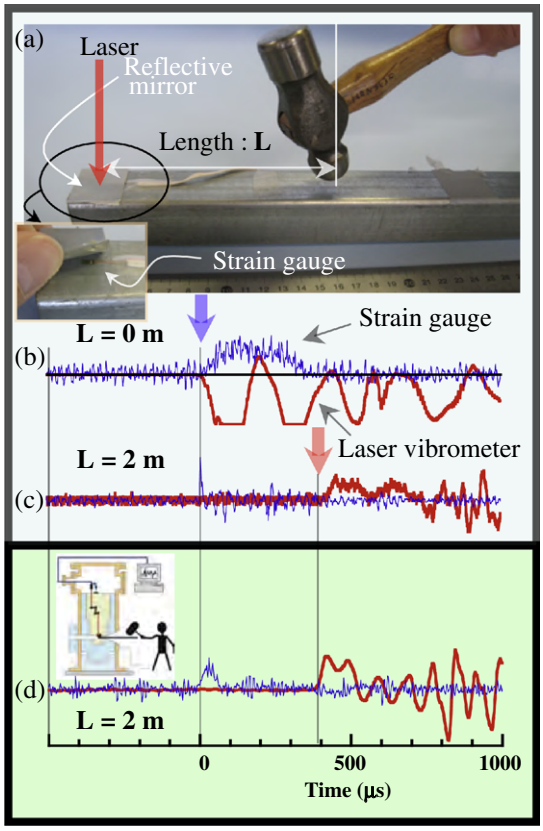

Fig. 9. Time response measurement of laser vibrometer in off-beam-line test. It was measured by striking hollow-pillar-steel-rod using hammer. Two sensors (strain gauge and reflective mirror for laser vibrometer) were arranged at same position to measure different wave motion (longitudinal and transverse wave) caused by hammer (a). Beginning time of strain gauge was used as a trigger. Measured time response are shown for two different striking positions (0 m and 2 m) (b) and (c) by He–Ne (632.8 nm) laser vibrometer. About 400 μs time delay was found due to difference propagation of wave motion. The time response was also measured by Nd-YAG (533 nm) laser vibrometer at actual target insertion hole (d). Same hollow-pillar-steel-rod with two sensors was used for the measurement. Same delay time was observed for 2 m striking position.

as shown in Fig. 9a. We measured a beginning time of each sensor for different striking positions (0 m and 2 m). In the measurement, the strain gauge was used for a trigger. As shown in Fig. 9a and b, about 400 μs time delay was observed by using the laser (He–Ne, 632.8 nm) vibrometer (Onosokki LV1720) due to the different propagation speed of wave motion. The time response for target vessel diagnosis system (Nd-YAG, 533 nm) was also measured using same hollow-pillar-steel-rod attached with two sensors, which was inserted into actual target insertion hole as shown Fig. 9d. It can be seen that same delay time was observed for 2 m striking position. This means that the validity of data taking system is confirmed in the time response.

3. First measured data

A first proton beam with energy of 3 GeV was irradiated into a mercury target on 30 May 2008. This was called Day-1, which was a memorial day of the first neutron production in our target. The single pulsed proton beam with Gaussian profiles was imposed into the target. The numbers were 0.4 Tera protons (Tps)/pulse, which meant the power of 5 kW@25 Hz. The detailed incident proton beam profiles are shown in Fig. 10a. The vibration of the target vessel caused by the proton incident also could be detected by using this target vessel diagnosis system as shown in Fig. 10b. Only noise data were also detected in the measurement.

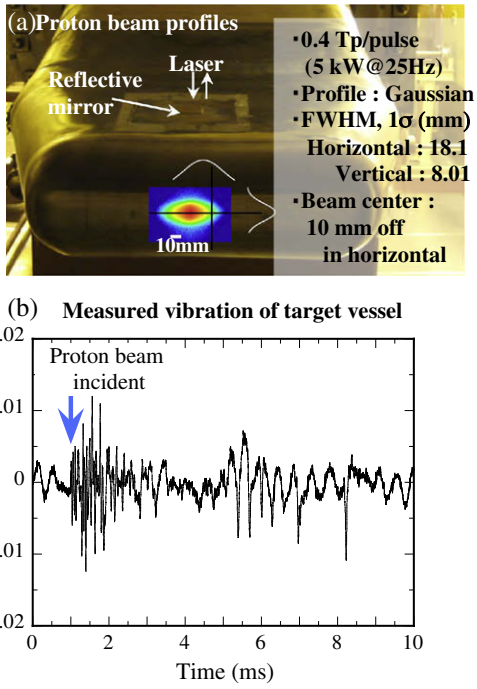

Fig. 10. First measured data taken by laser vibrometer and incident proton beam profiles. Incident proton beam profiles (a). Vibration of target vessel caused by proton incident also could be detected by using this target vessel diagnosis system (b).

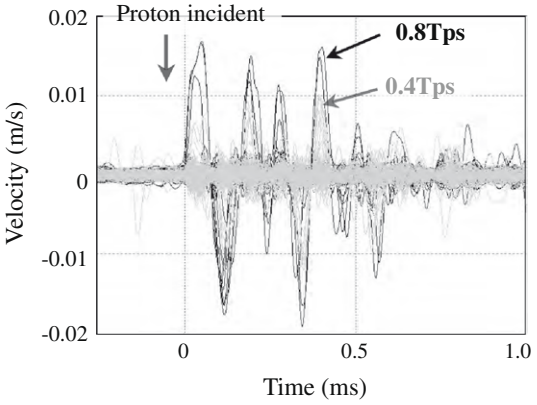

Fig. 11. Dependence on incident proton beam power in measured response data taken by vibrometer. Solid and grayed lines are case of incident numbers of protons, such as 0.8 and 0.4 Tera protons (Tps)/pulse, respectively. Many measured data are overwritten in the figure for easy comparison. It can be seen that higher power roughly gives higher amplitude.

3.1. Proton beam power dependence

Fig. 11 shows the measured data in the proton beam power per pulse. Many measured data are overwritten in the figure for easy comparison. It can be seen that higher proton beam power approximately gives higher amplitude in the figure. However, beam power and measured amplitude are not always correlated in all measured data. It seemed that the vibration data was in hiding in the much noise data.

3.2. Response measurement for different height proton beam injection

A beginning time (called delay time) of the response measurement was measured for the different height proton beam injection as shown in Fig. 12. Closing the proton beam to the mirror clearly

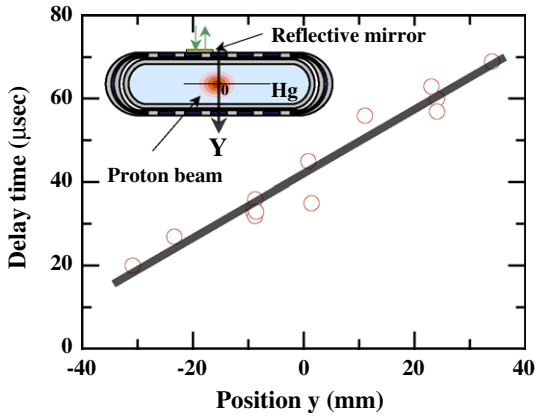

Fig. 12. Delay time measurement for different proton beam incident height. Beginning time (called delay time) of response caused by different height proton beam injection is measured. Proton beam was injected along vertical of target vessel cross section as shown in figure. Closing proton beam to reflective mirror clearly brought about shorter delay time.

brought about shorter delay time. Propagation velocity in the target also could be obtained by using the slope in the figure. The slope was decided by the linear curve fitting. The propagation velocity was ca. 1300 m/s, which was about 10% slower than that (1450 m/s) of liquid mercury. In the previous He-bubble-effect-study [12], even a small He bubble (size: ca. 10 mm) volume-fraction such as 10^{-6} could reduce about 10% of the propagation velocity of Hg. Such volume-fraction might be achieved easily in actual target system because it has a forced flowing mercury loop with a buffer tank filled with He (ca. 0.15 MPa).

4. Discussion

Sometimes, considerably noise can be seen in the measured data. It was not easy to distinguish the significant data such as including vibration, even providing filtering. It is considered due to two reasons. One is low returning laser beam intensity, just one order of magnitude larger in comparison with the background. The other is three layers structure of target vessel. The target vessel consists of Hg target vessel, He vessel and water shroud from inside. Each vessel is combined by the ribs and bolts with sealing by welding around the bolts as shown in Fig. 8a and b. The reflective mirror is joined on the water shroud but it is not be on the ribs directly due to the fabrication. This means that it is not direct vibration propagation, but indirect one through the ribs from Hg target vessel to the reflective mirror. In order to improve it, we consider to increase the reflection of the returned-laser-beam-intensity and modify the target structure. No-reflection area, which is about 20–30% in total, can be seen in the reflective mirror as shown in Fig. 8d because of the poor machining. We expect the large improvement by introducing the newly scratching technique in the micro machining process, resulting in one order of smaller machining such as several μm. Such R&D is in progress. We will also try to modify the target vessel structure in the 2nd target fabrication so as to propagate the vibration to the reflective mirror directly.

On the other hand, the performance loss of the reflective mirror might be brought by the irradiation damage, such as the embrittlement of the joining part, reduction of the fatigue strength due to the cycled stress, resulting in the exfoliation of the joining part. Not indirect machining method (micro machining and electroforming) but direct one on the surface of target container is desired to make the reflective mirror. We are going on developing the sub-milli milling technique in making many concave corners on the surface directly.

5. Conclusions

In order to utilize the laser Doppler vibrometer for the vibration measurement in the actual spallation source, we succeeded to develop the metal based (Ni) corner-cube retro-reflection (reflective mirror). Indirect machining method (convex machining and electroforming) enabled many small concaved corners (base size: around 200 μm). The Ni reflective mirror was installed on the target vessel (SS316L) by the vacuum Ag brazing. The reflection was reduced from 12.5% to 8.5% due to the re-crystallizing in the brazing process. However, the returned laser beam power from the target vessel surface at the beam incident position was 4–7 μW, which corresponded to the design value. The target vessel diagnosis system could be installed for the first time in actual pulsed spallation source and detected the vibration signal caused by proton beam bombardment.

Acknowledgements

The authors would like to thank the following people for their contributions: Dr. T. Fukai who belongs Nippon Engineering Industry & Service for the establishment of Ag brazing technique, Mr. K. Nakamura who belongs Mitsui Engineering & Shipbuilding Co., Ltd. for the installation of reflective mirror on the target vessel, Mr. N. Yoshida, H. Funatsu and S. Hisao who belong ONO SOKKI corporation for design and fabrication of the laser vibrometer and reflective mirror, Mr. J. Adachi who belongs Nagao Sangyo for the intermediary, Mr. A. Murai who belongs Technical-I Inc. for the installation of the data acquisition system and Mrs. S. Yoshinari who belongs JAEA for preparing of many pictures.

References

[1] S. Nagamiya, in: Proc. of Int. Conf. Radiation Shielding (ICRS9), J. Nucl. Sci. Technol. (Suppl. 1) (2000) 40.
[2] S. Nagamiya, Neutron News 16 (1) (2005) 16.
[3] Y. Ikeda, Newtron News 16 (1) (2005) 20.
[4] M. Futakawa, H. Kogawa, R. Hino, J. Phys. VI France 10 (Pt9) (2000) 237.
[5] J.R. Haines, K. Farrell, J.D. Hunn, D.C. Lousteau, L.K. Mansur, T.J. McManamy, S.J. Pawel, B.W. Riemaer, SNS-101060100-TR0004, 2002.
[6] K. Skala, G.S. Bauer, in: ICANS XIII, 1995, p. 559.
[7] M. Futakawa, K. Kikuchi, H. Conrad, H. Stechemesser, Nucl. Instrum. Methods A 439 (2000) 1.
[8] M. Futakawa, H. Kogawa, R. Hino, H. Date, H. Takeishi, Int. J. Impact Eng. 28 (2003) 123.
[9] M. Futakawa, T. Naoe, H. Kogawa, C. Tsai, Y. Ikeda, J. Nucl. Sci. Technol. 40 (2003) 895.
[10] M. Futakawa, T. Wakui, H. Kogawa, Y. Ikeda, Nucl. Instrum. Methods A 562 (2006) 676.
[11] M. Futakawa, H. Kogawa, S. Hasegawa, Y. Ikeda, B. Riemer, M. Wendel, J. Haines, G. Bauer, T. Naoe, K. Okita, A. Fujiwara, Y. Matsumoto, N. Tanaka, J. Nucl. Mater. 377 (2008) 182.
[12] S. Ishikura, H. Kogawa, M. Futakawa, K. Kikuchi, R. Hino, C. Arakawa, J. Nucl. Mater. 318 (2003) 113.